



ORIGINAL PAPER

CHARACTERISTICS OF THE FOUNDATION ROCKS USING GEOPHYSICAL TECHNIQUES: A CASE STUDY FOR THE EGYPTIAN SOLAR PLANT SITE, ASWAN, EGYPT**Abdelnasser MOHAMED^{*}, H. E. ABDELHAFIEZ and Sayed ALI***National Research Institute of Astronomy and Geophysics (NRIAG), 11421 Cairo, Egypt***Corresponding author's e-mail: nassermhmd@nriag.sci.eg*

| ARTICLE INFO | ABSTRACT |
|---|---|
| Article history: Received 29 April 2022 Accepted 20 June 2022 Available online 28 June 2022 | The main target of the present study is to investigate the foundation layers and the subsurface structures in an Egyptian solar plant site using geophysical techniques including the seismic refraction and Multichannel Analysis of Surface Waves (MASW). The studied solar park is situated at about 40 km to the north of Aswan city on the Aswan-Cairo highway road and is classified as the largest solar plant in Africa and worldwide. Due to its location in the vicinity of the most prone earthquake area in Egypt (Aswan seismic zone); it is imperative to mitigate the earthquake hazard in this region. The geophysical results show that the subsurface foundation in this site is primarily composed of two layers. The upper one is loose and incompetent soil sediments that extend down to about 10 m depth with P-wave velocity ranging from 400 to 1000 m/s and shear-wave velocity ranging from 260 to 550 m/s. The deeper section is considered the main foundation layer with velocities ranging between 650 and 1900 m/s and from 350 to 950 m/s for P-wave and shear-wave, respectively. The average shear-wave velocities calculated for the topmost 30 m (V_{S30}) vary almost between 319 and 834 m/s; thereby the studied site is primarily ranked into classes C&D (180-360 m/s & 360-760 m/s, respectively) according to the National Earthquake Hazards Reduction Program (NEHRP) soil classification. Additionally, the southwestern and southeastern zones of the site area are characterized by maximum velocity values, relative high values of rock densities, rigidity or shear modulus “ μ ”, Standard Penetration Test (N-Value), ultimate bearing capacity and allowable bearing capacity, while the low values are observed through the northern and middle sectors across the area. This study an integral part of many works being carried out delineating the subsurface foundation structures around the solar plant and allows the most appropriate sites for constructing the renewable energy plants to be sited away from the highly hazards prone areas. |
| Keywords: Shallow seismic refraction MASW Site characterization NEHRP | |

1. INTRODUCTION

It is very well known that each soil type responds differently when with the earthquake loading. As a result of significant earthquake such as those that have affected Mexico city (1985), San Francisco (1989), Los Angeles (1995) and Ahemadabad (2001), it has become apparent that the unconsolidated materials of young sedimentary basins can have a profound effect on the spatial distribution of ground motion amplification, resulting in variability in the severity of damage to buildings, transportation corridors and other lifeline infrastructures which includes the Solar Photovoltaic plant and the communication towers. So, site characterization is one of the important factors that control damage in urban areas from large and moderate earthquakes (Akin et al., 2016). The solar plant is one of the biggest solar projects in the world and located in Aswan area very close to the principal active seismic zone in this region. In this regard, it became of great interest for civil engineers to have knowledge of the characteristics of the soil and its spatial distribution

within the area to mitigate the earthquake hazard. In this investigation, two geophysical techniques (seismic refraction and multichannel analysis of surface waves (MASW) are applied to estimate the P- and SH-wave's velocity for site characterization. The investigation conducted at the solar photovoltaic plant site was through the shallow seismic refraction technique. For site effect estimation, the shallow refraction method is taken into consideration as one of the extreme functional geophysical techniques, which can be conducted in engineering seismology field i.e., tunnels, dam sites, landslides, quarries, roads, reclamation lands, caves, and cavities. The main targets of the refraction approach are determining the depth of bedrock and ground water level recognizing the lithology type as well as the lateral and vertical modification in lithology. The evaluated seismic velocities can be used to provide information on lithology, structural features, rock material quality and geotechnical factors, that are very useful for building construction and different civil engineering objectives. More detailed information regarding the refraction

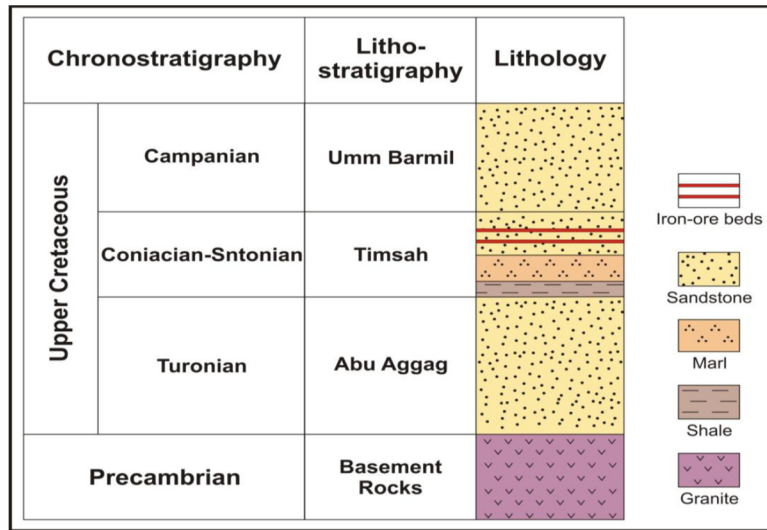


Fig. 1 Stratigraphic column of the study area (after Yousif, 2019).

tool is illustrated by Reynolds (2011). Many pioneers have utilized this approach to estimate the site properties, and the essential parameters for constructions in Egypt (e.g., Basheer et al., 2014; Mohamed et al., 2015; Mohamed, 2018). The MASW method (<http://www.masw.com>) is one of the exploration techniques used to compute the soil profile based on velocity (Park et al., 2002, 2007; Gjorgjeska et al., 2021). The MASW method can produce super resolution of spatial variability through a site. The principal advantages with such method are their non-destructiveness, non-invasive nature and relative speed of evaluation (Madun et al., 2016). There are many applications of acquiring seismic wave's data such as surface methods which can be applied for site investigation. The surface method is more versatile than different methods as it is not always constrained by any ground models and taking into consideration extra economical in terms of field operation (Matthews et al., 2000). The approach has been advanced and applied in civil engineering purposes, such as site characterization (Long and Donohue, 2007). The shear wave's velocity (V_s) is considered as a key factor in ground motion amplification and site effect analyses. In truth, micro-zonation is often based totally on the usage of the V_s inside the uppermost 30 m (V_{s30}), which is adopted by the National Earthquake Hazard Reduction Program (NEHRP) classification (<http://www.nehrp.gov>) in the USA.

2. GEOLOGIC AND TECTONIC SETTING

Many pioneers studied the investigated region and surrounding areas (e. g., Yousif, 2019; Mekkawi et al., 2008; Fat-Helbary and Mohamed, 2004; Hewaidy and Azab, 2002). Different geomorphic features are present in the study site; including hills, wadis and streams, dunes, the Nile River Valley, and the Nubian Plain. The Solar Plant is located within the Nubian Plain which extends from the Nile in the east to Gebel El-Barqa in the west. The Gebel El-Barqa is

one of the noticeable geomorphic features near the site location. The Nile River valley is located 17 km east of the Solar Park. Figure 1 summarizes the geological units at the area under investigation (Yousif, 2019). The study area is represented by five main rock units ranging from the Precambrian to Quaternary ages.

The Quaternary deposits in Aswan area have been distinguished into gravels, conglomerates, and clays. The recent deposits comprise a small portion of the surface of the study area and are represented by alluvial and Aeolian deposits. The alluvial deposits, sand and mud form the cultivated land in the eastern part of the study area. The Aeolian deposits are represented by blown-sand at the northern part of the area (Fig. 2).

From structural geology perspective, the area is deformed mainly by faults of different scales. The mapped faults are belonging to four prominent sets oriented in a descending order of frequency; ENE-WSW to E-W, NNW-SSE to N-S, NE-SW and NW-SE (Gaber et al., 2011).

The analysis of remote sensing data revealed the probability of the well-known Spillway Fault Zone to be extended to the Benban Solar Plant. The Spillway Fault Zone represents the longest fault in the area. The Spillway fault measures about 60 km length. It represents a fault zone that strikes towards the NNW direction where it extends from Nasser Lake to Benban Solar Park (Conoco, 1987; Fig. 2).

3. METHODOLOGY

3.1. SEISMIC REFLECTION TECHNIQUE

The basic requirements for the refraction technique are three components: a seismic source to generate elastic waves (the signal), several transducers (geophones) to detect the arrival of seismic waves at multiple points on the surface and a signal-enhancement data logger (seismograph) to control the survey and to record the data.

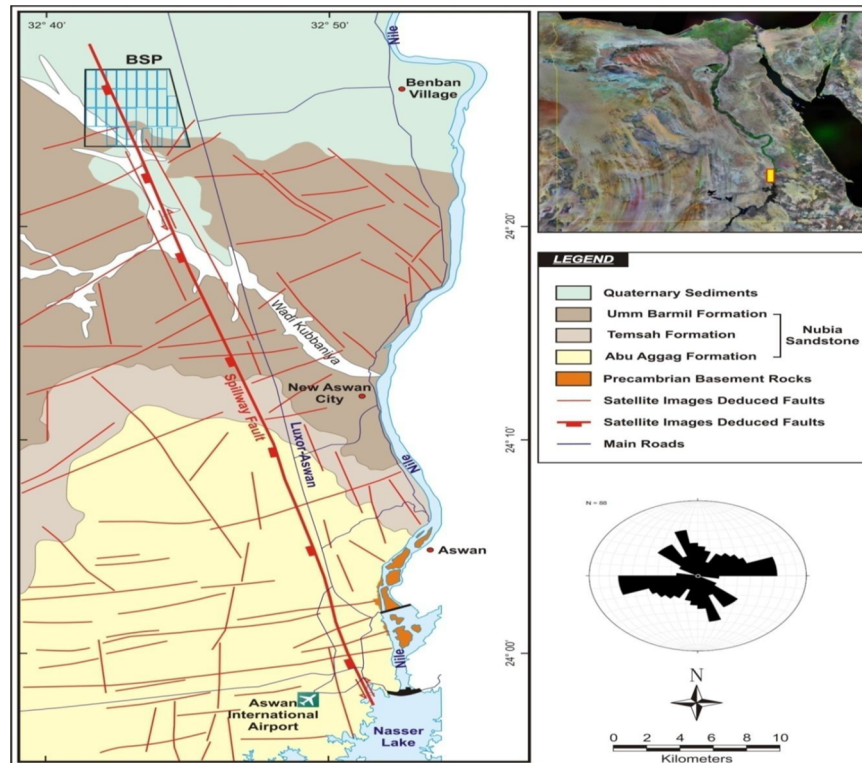


Fig. 2 Geological map of the study area showing rock unit distribution and the locations of major faults affecting the area; trend analysis of faults is provided by a rose diagram. (Note, BSP: Benban Solar Plant) modified after Conoco (1987).

The principal goal of using the source of seismic energy is to yield large enough signals into the ground to ensure sufficient depth penetration and high enough resolution to image the subsurface. In this investigation, the Geometric seismic source PWD-80 and 10 kg sledgehammer were utilized. Strata Visor-NZ seismograph has been used for the present study (Fig. 3). The system contains 48 detectors; each detector consists of a coil and a magnet, one rigidly attached to the frame and the other suspended from a fixed support by a spring. The Strata Visor-NZ employs a new concept in portable exploration seismograph. Also, the 14 Hz natural frequency vertical (P-waves) geophones were used to detect the wave's arrival times. A geophone cable is a multi-conductor cable with connectors connected at intervals along the cable. There is a standard cable used for refraction surveys, consisting of 24 takeout (geophone connections) at selected intervals. With the Geometrics Strata Vizion-NZ 48 channels seismograph, P- wave's profiles were measured in the ongoing project. The main use of the tool is to get 2-D cross section at the selected sites covering the study region with the wave's velocity and the sediments thickness. The outcomes of this technique will be used to calculate the geotechnical parameters across the Solar Photovoltaic plant site.



Fig. 3 The used seismograph (Geometrics Strata Vizion-NZ).

3.1.1. DATA ACQUISITION

The field survey is carried out at 82 selected sites (Fig. 4) indicating the refraction shot points distributed across the Solar plant's area for estimating of the seismic velocities and evaluating the ground model in order to characterise the lithology and the subsurface structures for the shallow layers. The data acquisition was performed through applying the forward (a 5 m distance from the first geophone), 1 inline (middle' in-

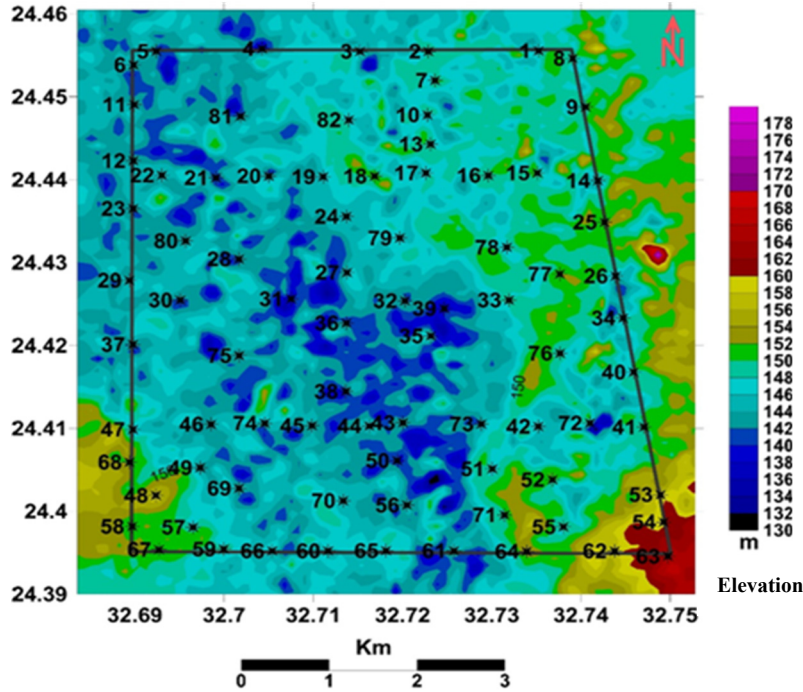


Fig. 4 Surface map of the topography the study area indicating the shot points across the solar plant site.

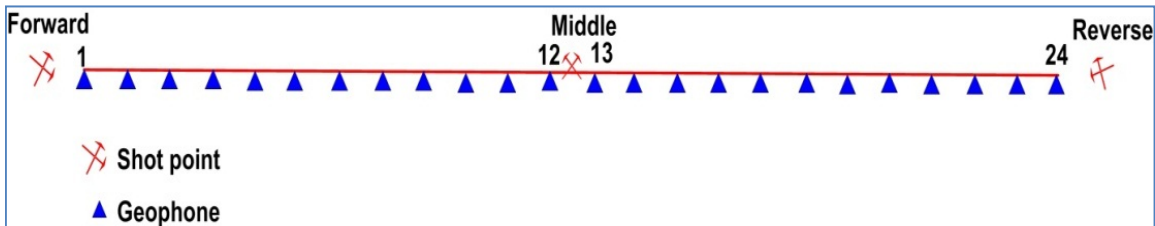


Fig. 5 Geophone spread for a refraction method with shot locations indicated.

between geophone 12 and 13), and reverse (a 5 m distance from the last geophone) shooting system using 10 kg sledgehammer (Fig. 5). Twenty-four geophones were laid out with fixed geophone spacing of 5 m interval and total spread of 120 m long. The data was acquired with a sample interval of 0.25 ms and a total recording length of 0.75 sec.

3.1.2. REFRACTION DATA ANALYSIS AND INTERPRETATION

The recorded seismic signals have been processed using the SeisImager™ program (<http://www.geometrics.com/software/seisimager-2d/>) a complete seismic data analysis and modeling software. The waveforms for P- waves obtained for every shot were analyzed by picking the first arrivals. The outputs indicated that almost all the subsurface sections probed are composed of two zones except some sites have three. Figures 6, 7 and 8 are the representative diagrams of the 2-D cross section at the study region with two- and three- layer models.

The calculated P wave velocities for the both surface and foundation layers at every line are computed and represented in 2-D maps as illustrated in Figures 9 and 10 respectively. From these maps, the

maximum average velocity of the P-wave at the first or surface layer is about 1,000 m/sec at the southeastern corner, while the minimum is about 400 m/sec at the middle and northern zones of the area. The maximum P-waves velocity of the second (foundation) layer is about 1,900 m/sec at the southeastern and southwestern parts, while the minimum value is reached to 650 m/sec for P-wave at the northern part of the plant site.

Based on the geological situation in and around the area, which mainly composed of Quaternary sediments (Fig. 2), the first layer (recent sediments) is made of wadi deposits mainly sand with average P- wave velocity about 581 m/sec. The second (intermediate) layer is the predominant layer represents the establishing strata in most of the area and mainly consists of sand and gravel with average velocity 840 m/sec for the P-wave, and average depth ranges from 2 to 18 m. The bedrock (3rd) layer appears only in some sites especially at the southern part of the solar plant and is mainly formed from sandstone with shale and clay, the average P-wave velocity is about 1,516 m/sec, so the most plant area did not extend into the third layer due to the large thickness of the second layer.

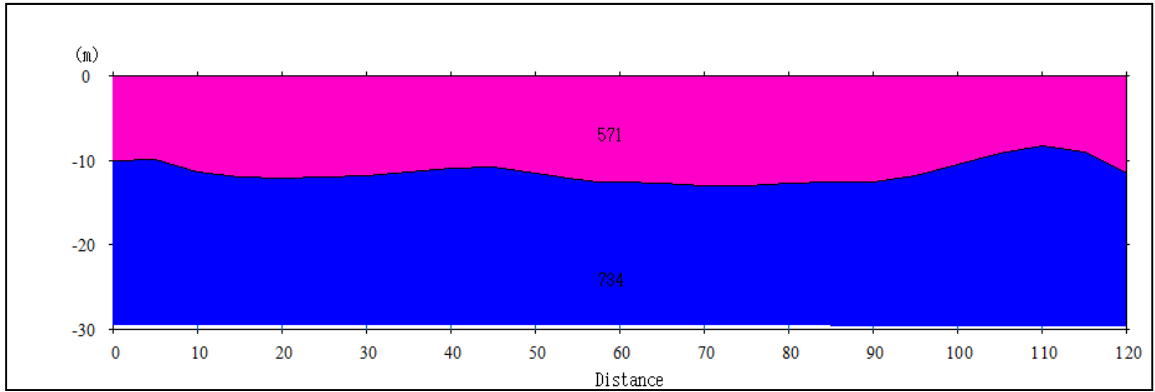


Fig. 6 The corresponding 2-D subsurface model with two layers at site 1.

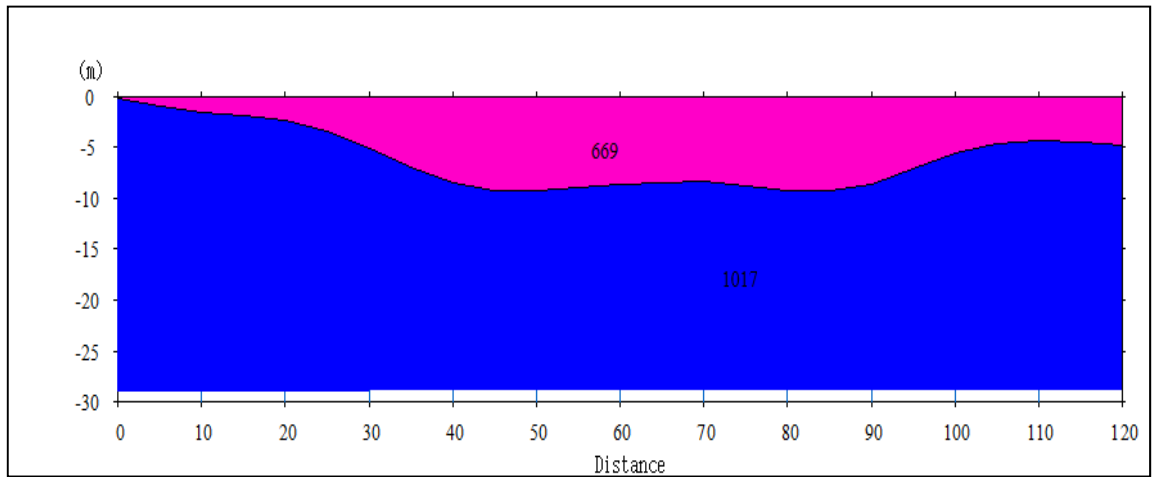


Fig. 7 The corresponding 2-D subsurface model with two layers at site 20.

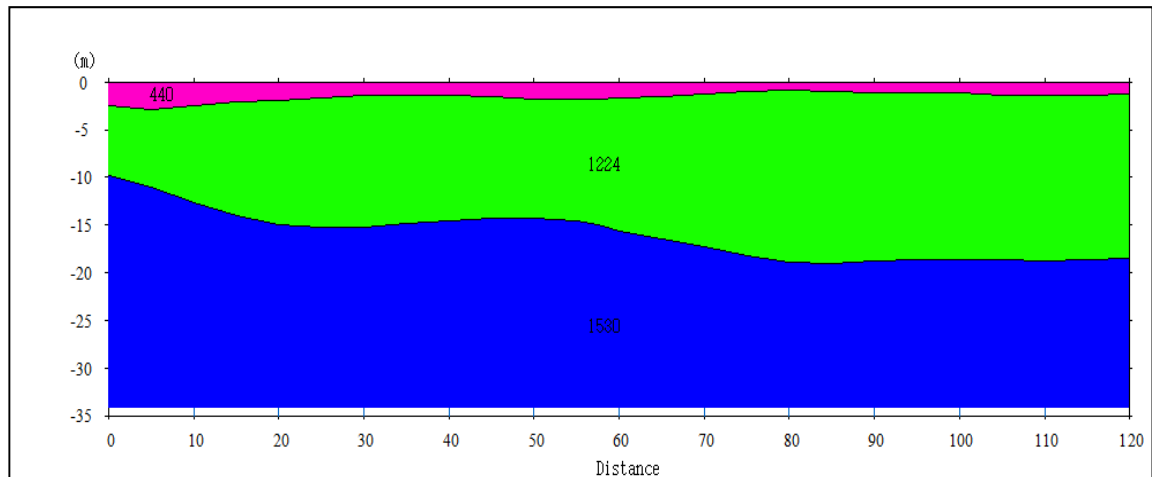


Fig. 8 The corresponding 2-D subsurface model with three layers at site 47.

3.2. MULTICHANNEL ANALYSIS OF SURFACE WAVE (MASW) TECHNIQUE

MASW method utilized the same seismograph utilized with refraction survey, but with different frequency range for the geophones. In our study, both the 1-D and 2-D MASW surveys were performed in many representative localities using Geometrics strata vizor-NZ instrument as a data logger for the shear wave (SH-wave) velocity profiles and the corresponding (V_{s30}). MASW is primarily based on

the inversion of the Rayleigh wave dispersion curves, which are proved to get the properties of the local S-wave velocity profile with a good accuracy. In this study, the preliminary depth version was estimated through a traditional seismic refraction measurement at each site of interest. The V_s profiles can be used in combination with seismic input motion to obtain site response and amplification spectra at the studied sites.

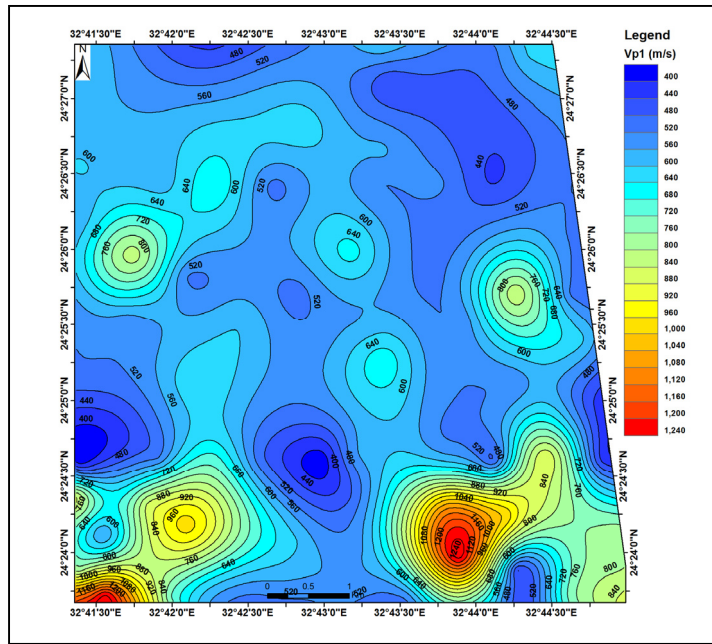


Fig. 9 P-waves velocity map of first layer.

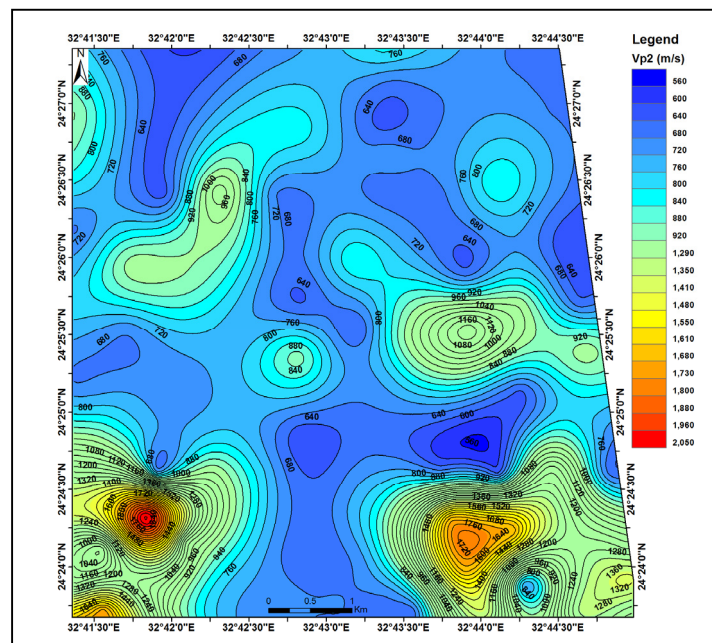


Fig. 10 P-waves velocity map of second (foundation) layer.

3.2.1. MASW DATA ACQUISITION (FIELD MEASUREMENTS)

For data acquisition, geophones are coated up in a straight line on the ground of the test location. As the geophones only record vertical motion, it is important that they are to be placed vertically on the ground.

Enhancement seismograph Strata Visor-NZ 48 channels along with low frequency 4.5 Hz vertical geophones were employed for the MASW method. The geophones are connected to a data acquisition card and a computer equipped with the necessary software. The geophones recorded the surface waves

that are produced by an impulsive seismic source. The geophones are lined up at 2 m interval with the source offset is 4 m. The recording length is 1.5 second and with sampling interval of 1ms. The used energy source for generating elastic waves was sledgehammer (10 kg) struck on a metallic plate. The data of every shot is recorded (Fig. 11) and saved by the equipment (Strata Visor-NZ seismograph). In 2D MASW technique, standard roll along the profiles is done in the field (Fig. 12). To reduce background noise and prevent interference with resolution and accuracy of the data, the acquisition conducted through hitting the

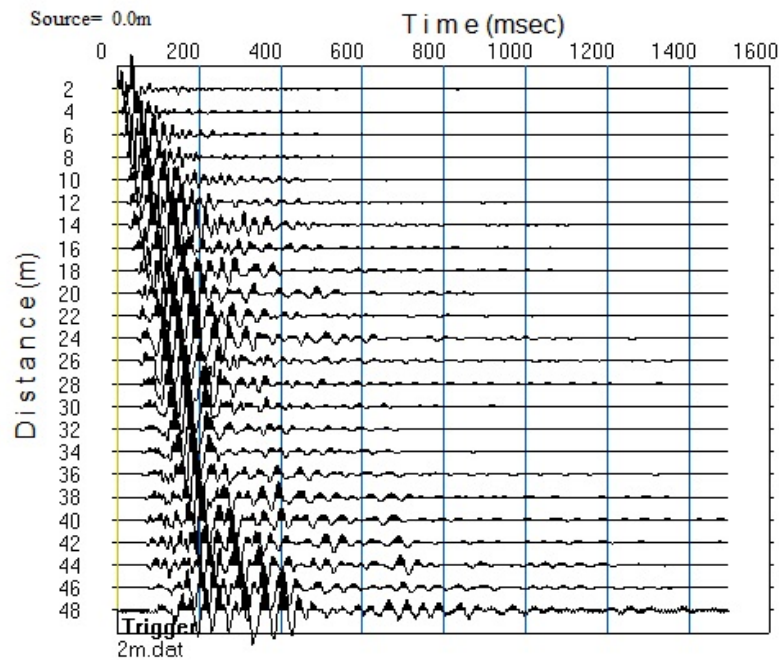


Fig. 11 A representative model of the active source multichannel records (MASW).

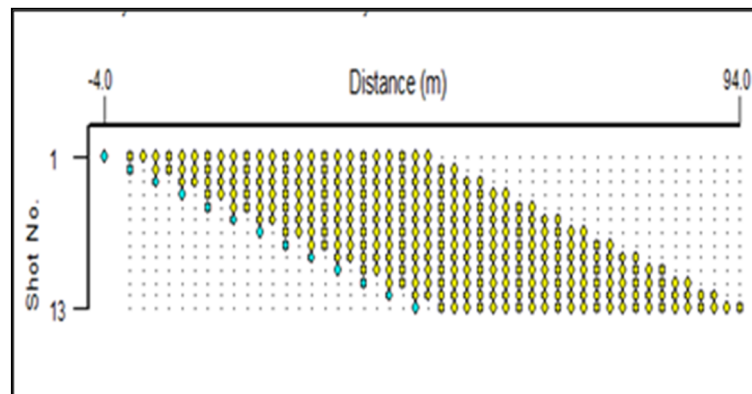


Fig. 12 Standard roll along of 2D MASW field work technique, Teal blue Circle: shot points, Yellow Circle: geophone locations.

striker plate during periods of periods of silence of traffic and quiet and simple wind.

3.2.2. MASW DATA ANALYSIS

The seismic raw records were processed with SeisImager/SW software. The procedure of MASW includes three steps: 1) measurement of seismic surface waves produced from different varieties of seismic sources (e. g. sledgehammer), 2) evaluation of the surface wave phase velocities (by drawing out the fundamental-mode dispersion curves, one curve from every signal), and 3) obtaining 1D (depth) V_s profiles by inverting these curves (Park et al., 1999). Figure (13a) shows the raw wiggle plot got from the field test. The recorded seismic waves were analyzed to generate phase velocity images in frequency domain (Fig. 13b).

3.2.3. RESULTS OF MASW AND DISCUSSION

The MASW method emphasized the minimization of near field and far-offset effects, acquisition speed, sampling redundancy, and ensures overall data accuracy. The V_s layer velocities and thicknesses are necessary to the seismologists and engineers, particularly within the site effect modelling. The output results of the current study provides several important factors such as: V_s values calculated using the observed velocity-depth profiles, V_{s30} and site class according to NEHRP site classification. The MASW approach was performed at 82 sites.

The MASW profile outputs, 1D and 2D SH- velocity models are clarified in Figures 14, 15, 16 and 17 respectively. Generally, most of the MASW profiles show two layers of different soil SH-velocity rigidity. The top layer which starts from ground

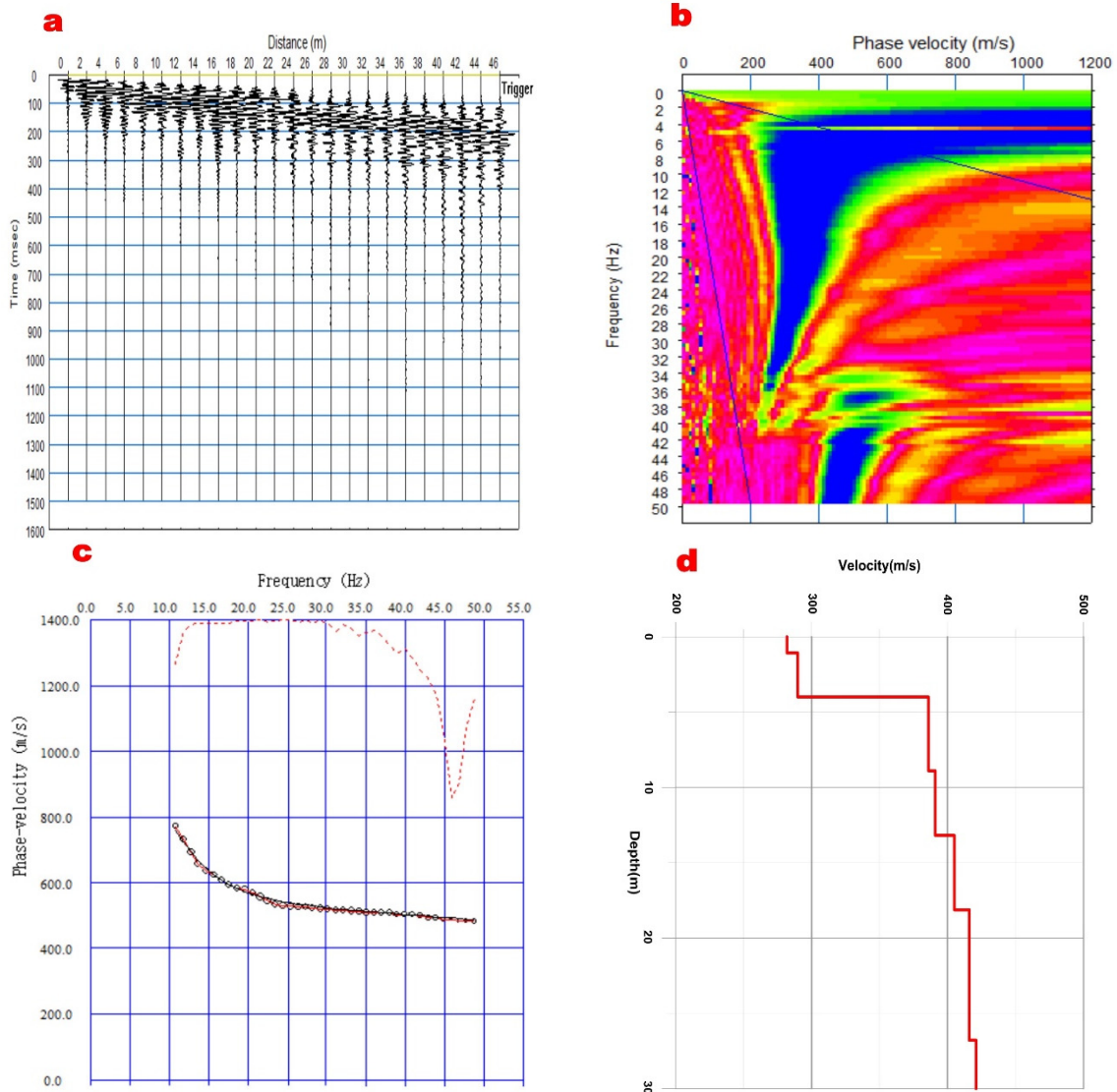


Fig. 13 MASW data analysis procedure with SeisImager, a) detection of surface waves, b) image of dispersion curve, c) dispersion curve inversion, d) 1D shear velocity profile.

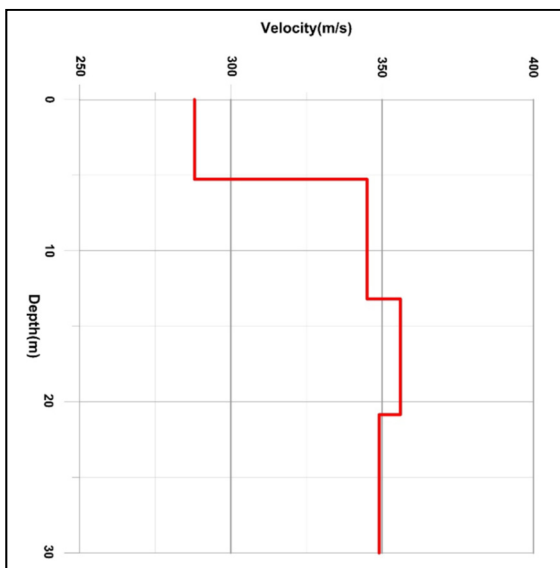


Fig. 14 1D shear velocity V_s curve obtained from the MASW at site 6.

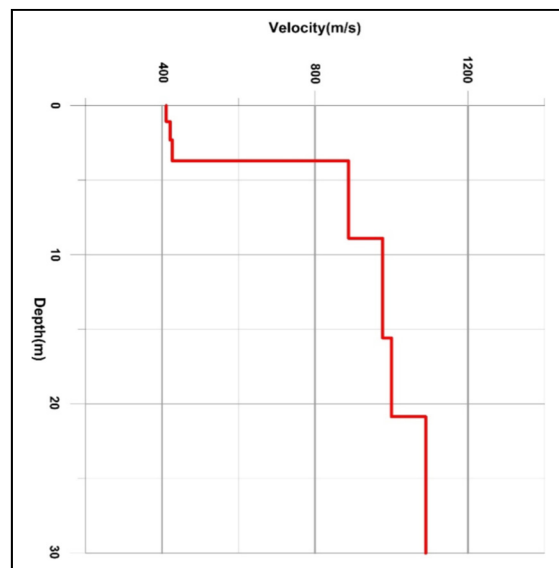


Fig. 15 1D shear velocity V_s curve obtained from the MASW at site 49.

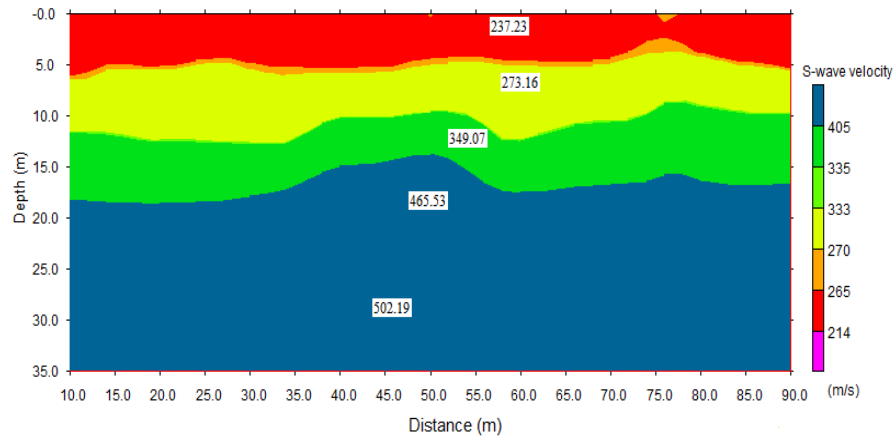


Fig. 16 2D shear wave velocity profile at site 28.

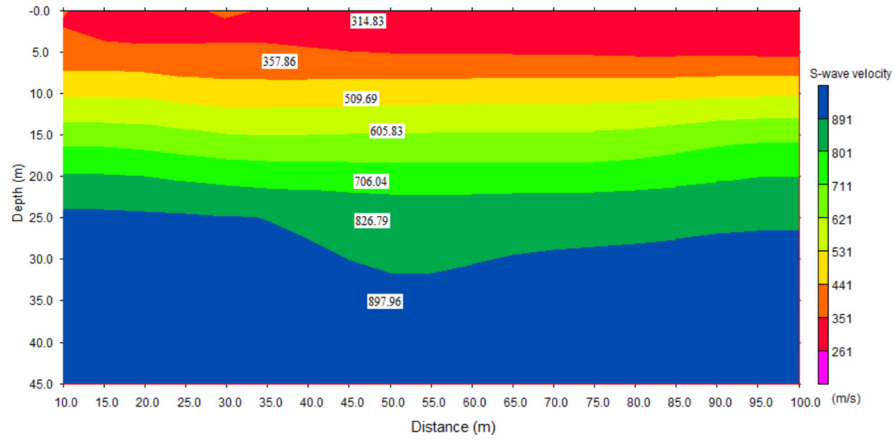


Fig. 17 2D shear wave velocity profile at site 63.

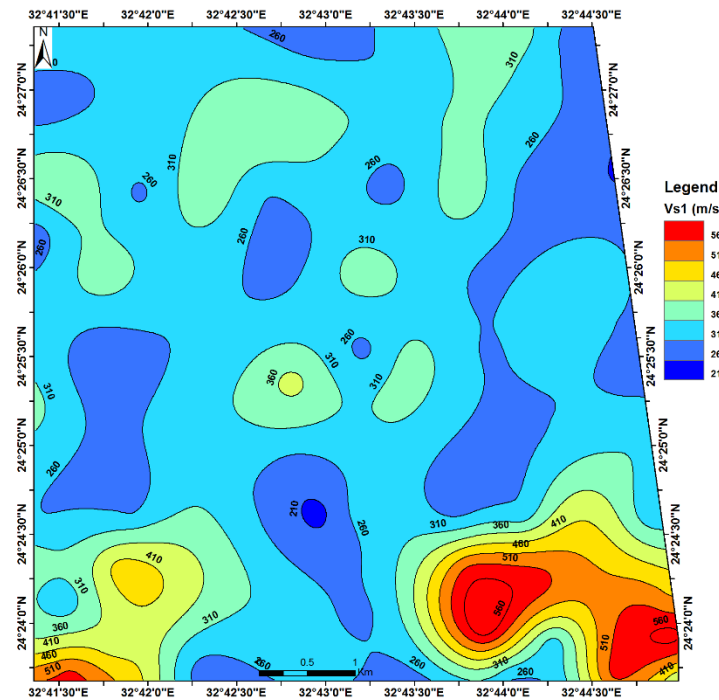


Fig. 18 Shear wave velocity map of surface layer.

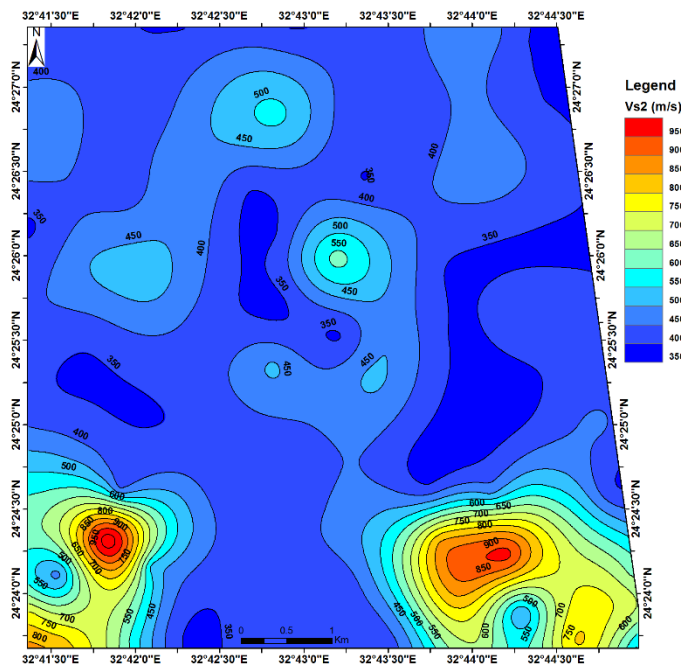


Fig. 19 Shear wave velocity map of the second (foundation) layer.

Table 1 Definition of NEHRP provisions (BSSC, 2003) in terms of V_{S30} .

| Site Class | Rock/soil description | Range of V_{S30} (m/s) |
|------------|--|-----------------------------|
| A | Hard rock | $V_{S30} > 1500$ |
| B | Rock | $760 < V_{S30} \leq 1500$ |
| C | Very dense soil and soft rock | $360 < V_{S30} \leq 760$ |
| D | Stiff soil | $180 \leq V_{S30} \leq 360$ |
| E | Soft soil, | $V_{S30} < 180$ |
| F | Special soils requiring site-specific evaluation | ----- |

surface and extends to depth ranging from 2 to 18 meters shows relatively low V_s (204–570 m/s). The next layer to this layer has relatively moderate V_s (336–977 m/s) some profiles show three layers where the 3rd layer has velocity from 766 to 946 m/s. The calculated shear wave velocities for the both two layers at every line are computed and represented in 2-D maps as illustrated in Figures 18 and 19 respectively.

4. V_{S30} AND SITE CLASSIFICATION

The near-surface material's elastic properties and their impact on the seismic wave propagation are very crucial in the fields of earthquake geotechnical engineering, civil engineering, and environmental earth science. The seismic site characteristics for computing the earthquake hazard is generally done depending on the near-surface shear velocity values. The average shear-wave velocity of the top 30 m of the earth (V_{S30}) is a significant factor used in classifying sites in recent constructing codes (e.g., BSSC, 2001; IBC, 2009).

The site classification derived on the basis of V_{S30} estimated from shallow shear-wave velocity models are also important in deriving strong-motion

prediction equations, in construction of maps of National Earthquake Hazard Reduction Program (NEHRP) site classes, and in applications of building codes to specific sites. This method was adopted by the Building Seismic Safety Council (BSSC, 1998) in the NEHRP recommended provisions for seismic assizes. The classification of the 82 MASW selected profiles in the plant area was established following the NEHRP (2001) guidelines (Table 1) based on V_{S30} . The V_{S30} is derived from the following equation:

$$V_{S30} = \frac{30}{\sum_{i=1,N} \frac{h_i}{v_i}} \quad (1)$$

Where h_i and v_i are the thickness and velocity of the layers between 0 and 30 m, respectively. The average V_s estimated for the topmost 30 m vary almost between 319 m/s and 834 m/s (Fig. 20). Based on NEHRP, site classes C&D are predominant in the solar plant region.

Calculation of the geotechnical factors for the shallow sedimentary layers of the soil and bedrock mechanical properties are of special importance for civil engineering works. Refraction is a technique developed not only for determination of layer velocities and thickness, but also for assessment of soil

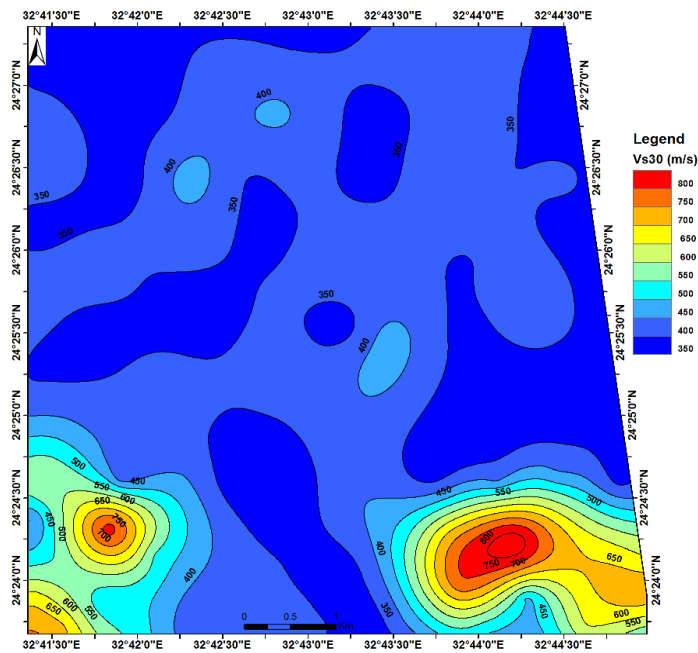


Fig. 20 The classification of the V_{s30} over the tested area.

and rock material goodness and geotechnical parameters, which are very useful for new communities and other civil purposes. The velocities of shear and compressional-waves acquired from the refraction profiling and MASW profiles were used for estimating the geotechnical factors and dynamic characteristics for the shallow sedimentary layers, which are of great significance in engineering applications as in the following calculations:

1. Bulk Density (ρ): The compressional wave velocity can be utilized for material densities

evaluation. This empirical relationship is valid for sedimentary rocks and shows the raise in P-wave velocity (V_p) with density (ρ) (Gardner et al., 1974):

$$\rho = aV_p^{1/4} \quad (2)$$

(a) is a constant equivalent to 0.31 when the density is in g/cm^3 and V_p is in m/s. The southwestern and southeastern zones are recognized by relative high rock densities (Figs. 21 and 22).

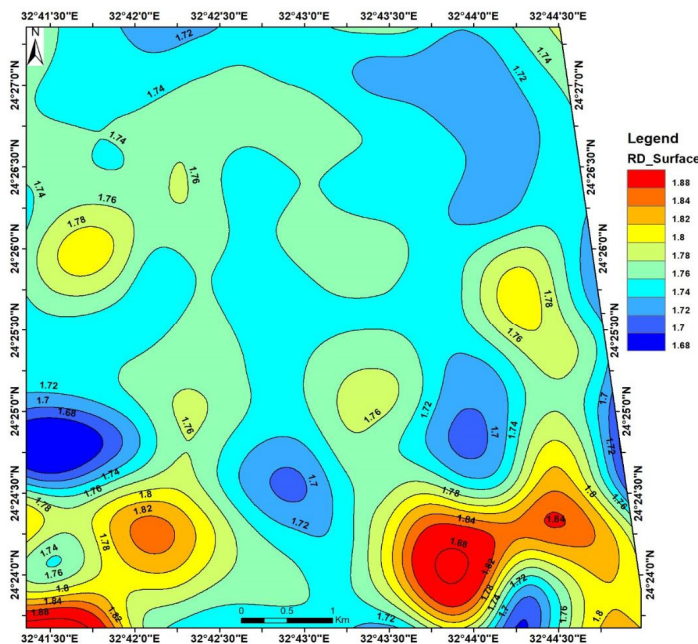


Fig. 21 The Bulk Density distribution for the first layer.

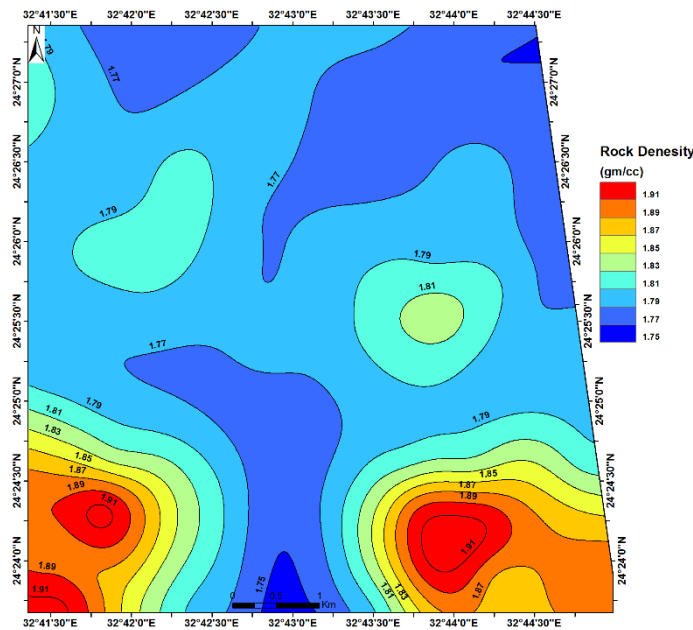


Fig. 22 The Bulk Density classification for the foundation layer.

2. Shear Modulus (μ) or Rigidity: The shear modulus, usually abbreviated (μ), is the ratio among shear stress and shear strain and plays the same role in describing shear as Young’s modulus does in describing longitudinal strain. Shear stress cannot be applied to ideal liquids and gases. For these substances $\mu = 0$. Only solids possess the physical characteristics described by the shear modulus. The shear modulus may be addressed in terms of (V_s) Sharma (1978):

$$\mu = \rho V_s^2 \tag{3}$$

The southeastern and southwestern zones are recognized by high values of the rigidity (Figs. 23 and 24).

3. Standard Penetration Test (SPT) [N-Value]: The resistance to penetration by normalized cylindrical bars under standard load, is known as the Standard Penetration Test (SPT), and can be determined based on Imail et al. (1976) formula and (Stümpel et al., 1984) as follow:

$$V_s = 89.9 N^{0.341} \tag{4}$$

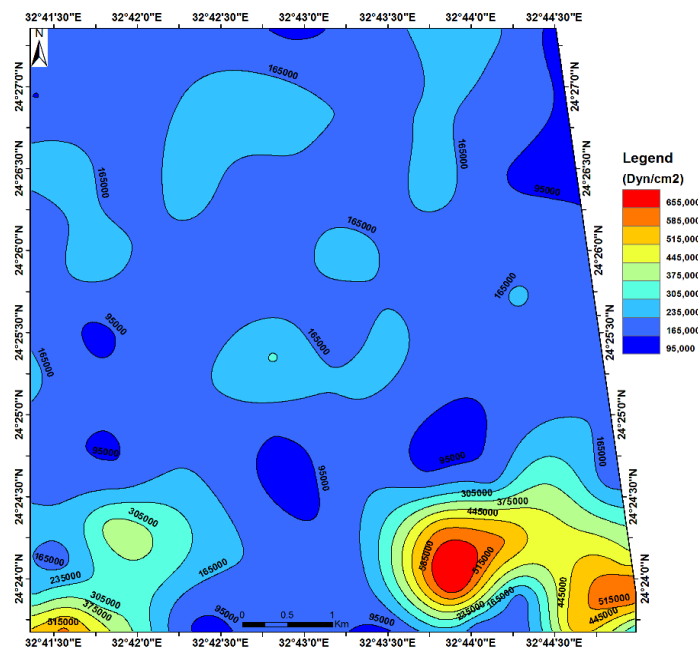


Fig. 23 The shear modulus classification through the surface layer.

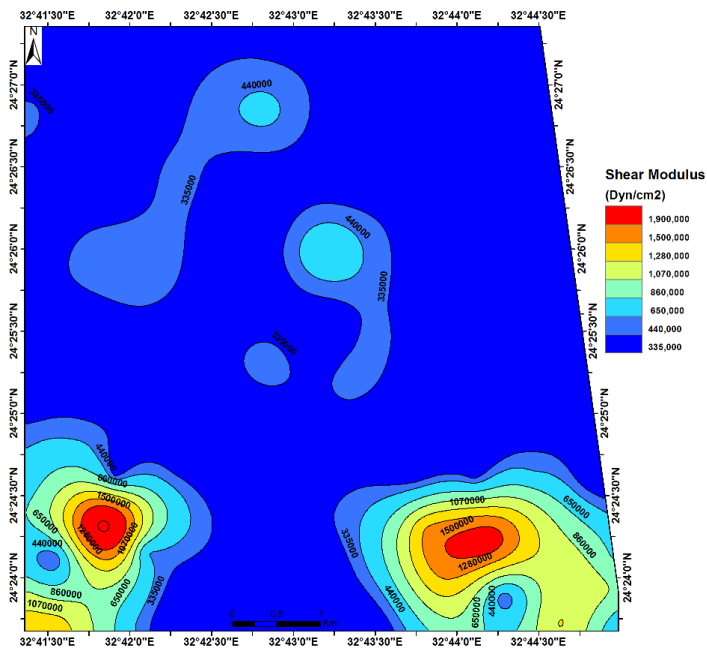


Fig. 24 The shear modulus map for the foundation layer.

Where V_s is the horizontal shear velocity. The southeastern and southwestern parts are characterized by high N-Value (Figs. 25 and 26).

4. Foundation material-bearing capacity at subsurface deposits can be summarized as following:

The ultimate bearing capacity (Qult): The ultimate bearing capacity of the foundation material is the required maximum load for shear failure. The controlling parameter of the ultimate bearing capacity of the soil is the shear strength. The ultimate bearing

capacity of cohesionless soils utilizing the SPT can be calculated by applying the formula established by Vesic (1974):

$$\text{Log Qult} = 2.932 (\log V_s - 1.45) \quad (5)$$

Figures (27 and 28) illustrate the ultimate bearing capacity distribution over the region; the relatively low values are recognized in the northern and middle zones of the area, indicating a relatively incompetent soil. The highest values are found in southeastern and southwestern sectors of the solar plant area.

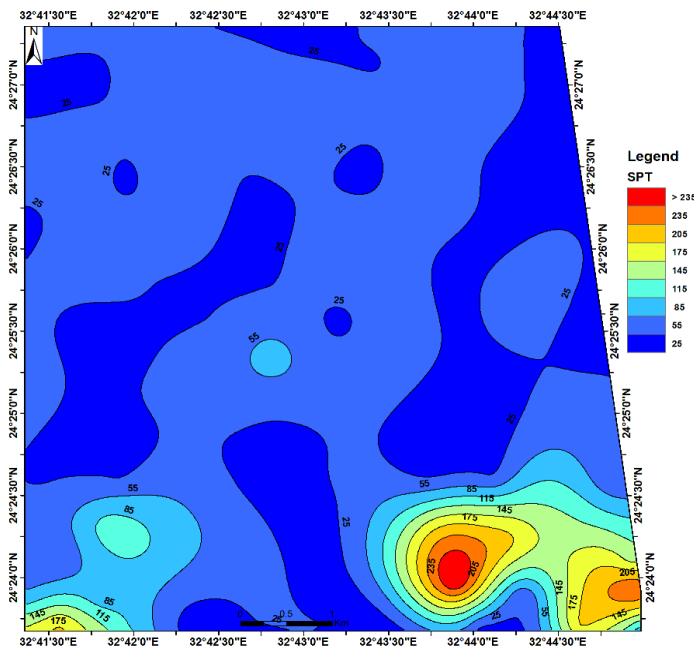


Fig. 25 The N-Value distribution for the surface layer.

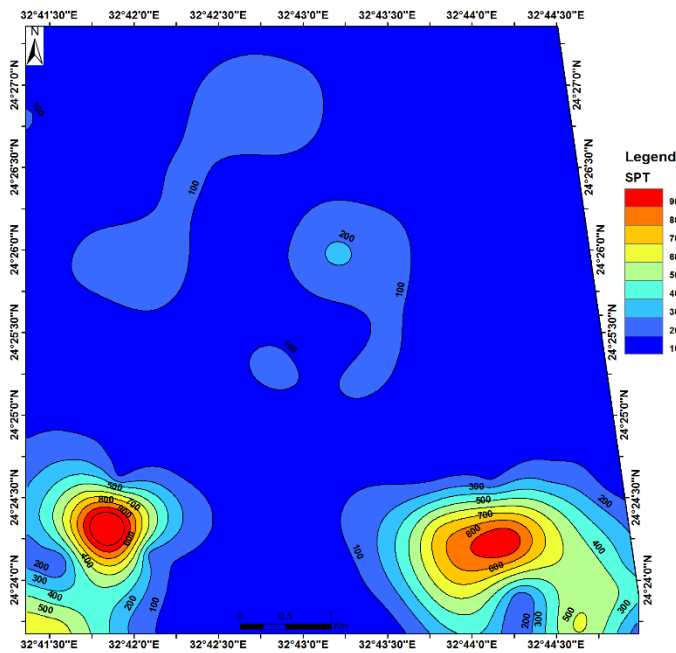


Fig. 26 The N-Value map across the foundation layer No. 2.

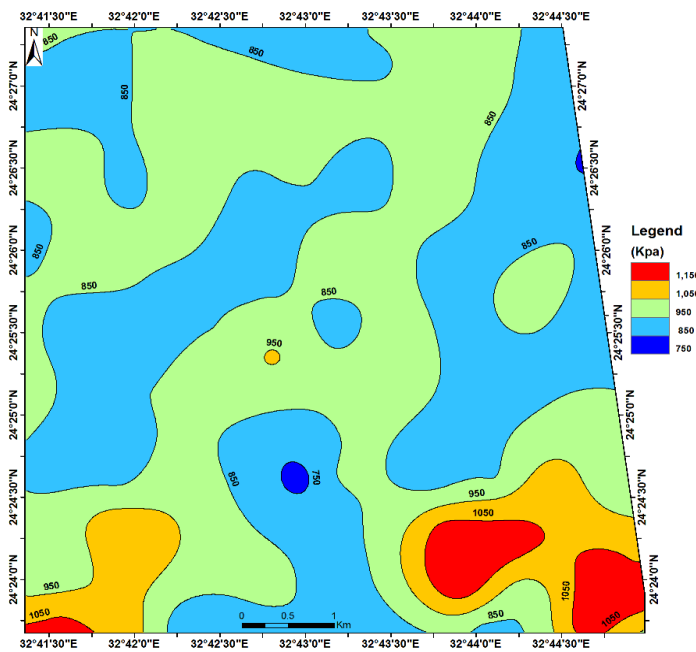


Fig. 27 The distribution of the ultimate bearing capacity across the surface layer.

The allowable bearing capacity (Q_{all}): Before designing the buildings, the allowable bearing capacity should be considered. It can be acquired using the ultimate bearing capacity value by dividing on a suitable parameter of safety (F), Parry's formula (1977) as:

$$Q_{all} = Q_{ult}/F \tag{6}$$

The safety parameter equals 2 and 3 for the cohesionless and cohesive soils, respectively (Figs. 29 and 30), the relatively low values are recognized across the northern and middle parts of the area,

indicating a relatively incompetent soil. The highest values are found in the southeastern and southwestern parts. Integration among different engineering, elastic, consolidation, and strength parameters proves a good competent of the second layer at the southeastern and southwestern sectors of the area. Therefore, this layer is likely suggested as the most acceptable zone for foundation aims at these sites.

5. CONCLUSIONS

The refraction profiles for P- and shear waves have been acquired covering the studied plant's site.

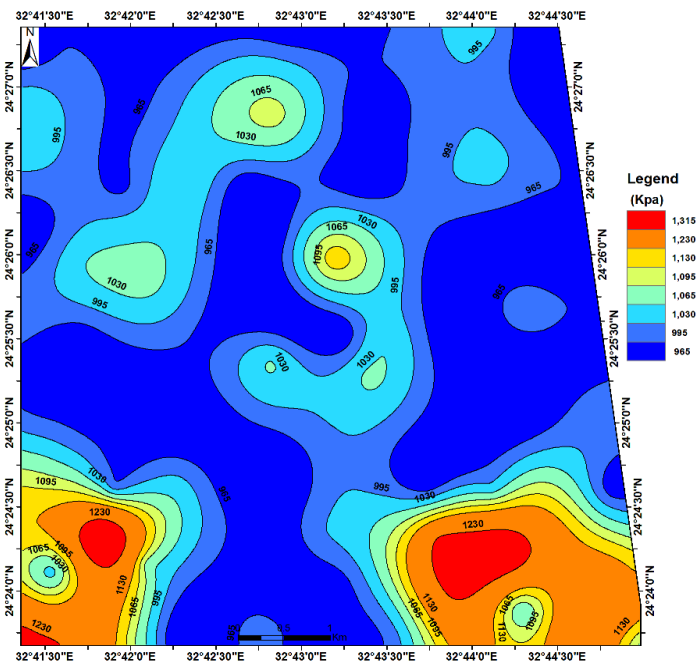


Fig. 28 The ultimate bearing capacity distribution at the foundation layer.

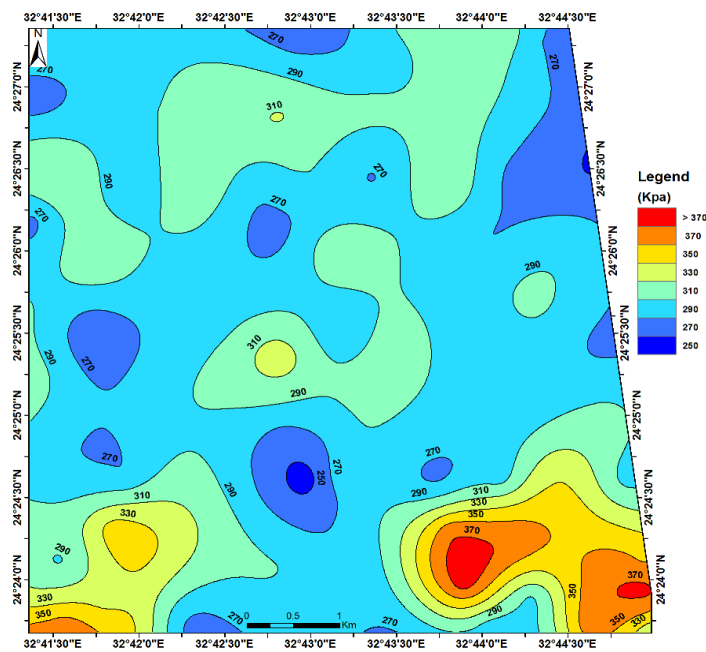


Fig. 29 The allowable bearing capacity map through the upper layer.

The outcomes indicated that the most of the area occupied with two layers (surface and foundation) except some sites have three layers. P-waves velocity across the area ranged from about 400-1000 m/s and the shear waves velocity from 260 to 550 m/sec for the uppermost layer. The maximum velocities values were detected at the southern part in particular to the eastern and western corners, while the minimum values were measured at the northern and central parts.

The deeper layer is considered the main foundation layer with velocities ranging between 650 and 1900 m/sec and from 350 to 950 m/sec for P-wave and shear-wave, respectively. The maximum values noticed at the southeastern and southwestern corners while the minimum at the northern and the central layers. MASW profiles show two layers, the upper layer which starts at the ground level and extends right down, up to depth from 2 to 18 m, shows relatively

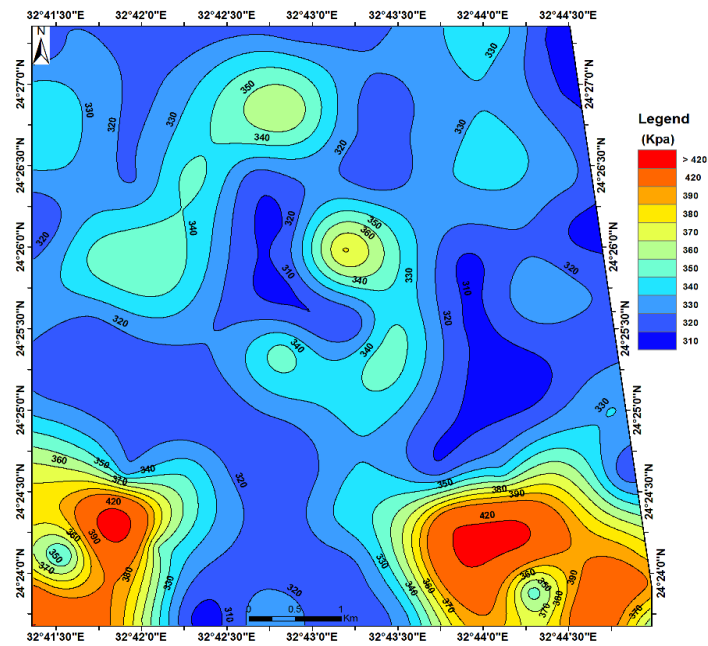


Fig. 30 The distribution map of the allowable bearing capacity through the construction layer.

low V_s (204–570 m/s). This layer is underlying by the foundation layer of relatively moderate shear wave velocity (336–977 m/s); some profiles showed three layers where the 3rd one has velocity from 766 to 946 m/s.

The average V_s velocities computed for the topmost 30 m (V_{s30}) vary almost between 319 and 834 m/s. Based on NEHRP, site classes C&D are predominant across the plant region, expect two sites locate in site class B. The geotechnical factors (e.g. bulk density, shear modulus, N-value, the ultimate and the allowable bearing capacity) are computed using the refraction and MASW results. The southwestern and southeastern zones of the plant area are characterized by relative high rock densities, relative high rigidity, or shear modulus “ μ ” values, high N-Value, high ultimate bearing capacity and high allowable bearing capacity while the low values are observed through the northern and middle sectors across the area.

Integration of engineering, elastic, consolidation, and strength factors suggests a good quality of the foundation layer across the southeastern and southwestern zones. Consequently, this layer is probably proposed as suitable for the construction targets at these sites. This work is a perfect investigation study for delineating the subsurface foundation structures to check the most appropriate sites for constructing the renewable energy plants away from the highly hazards areas.

ACKNOWLEDGMENTS

The authors are very grateful to the Department of Seismology, NRIAG, Egypt, for providing this study with instruments for data acquisition.

Funding information: This project was supported financially by the Science and Technology Development Fund (STDF), Egypt (Grant No. 28992).

REFERENCES

- Abd El-Rahman, M., Setto, I. and El-Werr, A.: 1992, Inferring mechanical properties of the foundation materials at the 2nd Industrial zone city, from geophysical measurements. EGS Proc. of the 10th Ann. Meet, 50–61.
- Akin, M.K., Kramer, S.L. and Topal, T.: 2016, Dynamic soil characterization and site response estimation for Erbaa, Tokat (Turkey). Nat. Hazards, 82, 3, 1833–1868. DOI: 10.1007/s11069-016-2274-4
- Basheer, A.A., Abdelmotaal, A.M., Mesbah, H.S. and Mansour, Kh.K.: 2014, Application of geophysical methods for geotechnical parameters determination at New Borg El-Arab Industrial City, Egypt. Curr. Urban Stud., 2, 1, 20–36. DOI: 10.4236/cus.2014.21003
- BSSC: 1998, NEHRP recommended provisions for seismic regulations for new buildings and other structures. 1997 edition, part 2-Commentary, FEMA 303 Report, Building Seismic Safety Council, Washington D.C.
- BSSC: 2001a, NEHRP recommended provisions for seismic regulations for new buildings and other structures. 2000 edition, part 1-Provisions, FEMA 368 Report, Building Seismic Safety Council, Washington, D.C.
- BSSC: 2001b, NEHRP recommended provisions for seismic regulations for new buildings and other structures. 2000 edition, part 2-Commentary, FEMA 369 Report, Building Seismic Safety Council, Washington, D.C.
- BSSC: 2003, NEHRP recommended provisions for seismic regulations for new buildings and other structures. Accompanying commentary and maps, FEMA 450 Report, Building Seismic Safety Council, Washington D.C., 17–49.
- CONOCO: 1987, Geological map of Egypt. NG 36 SW LUXOR; Scale 1:500000.

- Fat-Helbary, R. and Mohamed, H.: 2004, Seismicity and seismotectonics of the West Kom Ombo area, Aswan, Egypt, *Acta Geodyn. Geomater.*, 1, 2 (134), 195–200.
- Gaber, A., Koch, M., Geriash, M.H. and Sato, M.: 2011, SAR remote sensing of buried faults: implications for groundwater exploration in the Western Desert of Egypt. *Sens. Imaging*, 12, 3-4, 133–151.
- Gardner, G.H.F., Gardner, L.W. and Gregory, A.R.: 1974, Formation velocity and density the diagnostic basics for stratigraphic traps. *Geophysics*, 39, 6, 770–780. DOI: 10.1190/1.1440465
- Gjorgjeska, I., Sheshov, V., Edip, K. and Bojadjeva, J.: 2021, Combined seismic methods for 3D modelling of quaternary deposits: Application to Skopje sedimentary basin. In: *Proc. 1st Croatian Conference on Earthquake Engineering, 1CroCEE*.
- Hewaidy, A.A. and Azab, M.M.: 2002, Paleocene gastropods and nautiloids of southwest Aswan, Egypt. *Egypt. Jour. Paleontol.*, 2, 199–218.
- ICC-IBC- International Building Code: 2009, International Code Council, USA.
- Imail, T., Fumoto, H. and Yokota, K.: 1976, P- and S-wave velocities in subsurface layer of ground in Japan. Urawa Research Institute, Oyo Corporation, Tokyo.
- Long, M. and Donohue, S.: 2007, In situ shear wave velocity from multichannel analysis of surface waves (MASW) tests at eight Norwegian research sites. *Can. Geotech. J.*, 44, 5, 533–544. DOI: 10.1139/t07-013
- Madun, A., Supa'at, M.E.A., Tajudin, S.A.A., Zainalabidin, M.H., Sani, S. and Yusof, M.F.: 2016, Soil investigation using multichannel analysis of surface waves (MASW) and boreholes. *ARPN J. Eng. Appl. Sci.*, 11, 6, 3759–3763.
- Matthews, M.C., Clayton, C.R.I. and Own, Y.: 2000, The use of field geophysical techniques to determine geotechnical stiffness parameters. *ICE Proc. Geotech. Eng.*, 143, 1, 31–42. DOI: 10.1680/geng.2000.143.1.31
- Mekkwawi, M., Abdel-Monem, S., Rayan, A., Mahmoud, S., Saleh, A. and Moustafa, S.: 2008, Subsurface structure and crustal deformation at Kalabsha fault, Aswan-Egypt, from magnetic, GPS and seismic data. *NRIAG J. Geophys. Special issue, Helwan, Egypt*, 681–700.
- Mohamed, A.: 2018, Geophysical/Geotechnical investigation for earthquake risk mitigation of the strategic and development projects, South Egypt. 12th International Conference on Civil and Architecture Engineering, 12, 12, 1–12. DOI: 10.21608/iccae.2018.30049
- Mohamed, A., Lindholm, C. and Girgis, M.: 2015, Site characterization and seismic site response study of the Sahary area, South Egypt. *Acta Geodyn. Geomater.*, 12, 4, 427–436. DOI: 10.13168/AGG.2015.0032
- Park, C.B., Miller, R.D. and Miura, H.: 2002, Optimum field parameters of an MASW survey. *Proc. 6th SEG-J International Symposium, Tokyo, Japan, Extended Abstracts*.
- Park, C.B., Miller, R.D. and Xia, J.: 1999, Multi-channel analysis of surface waves. *Geophysics*, 64, 3, 659–992. DOI: 10.1190/1.1444590
- Park, C.B., Miller, R.D., Xia, J. and Ivanov, J.: 2007, Multichannel analysis of surface waves (MASW)-active and passive methods. *The Lead. Edge*, 26, 1, 60–64. DOI: 10.1190/1.2431832
- Parry, R.H.G.: 1977, Estimating bearing capacity of sand from SPT values. *J. Geotech. Geoenviron. Eng.*, 103, 1013–1045.
- Reynolds, J.M.: 2011, *An introduction to applied and environmental geophysics*. Second Edition, John Wiley and Sons Ltd.
- Sharma, P.V.: 1986, *Geophysical methods in geology*. Second Edition. Elsevier, Oxford, New York.
- Stümpel, H., Kähler, S., Meissner, R. and Milkereit, B.: 1984, The use of seismic shear waves and compressional waves for lithological problems of shallow sediments. *Geophys. Prospect.*, 32, 4, 662–675. DOI: 10.1111/j.1365-2478.1984.tb01712.x
- Vesic, A.S.: 1974, Analysis of ultimate loads of shallow foundation: Closure of discussion of original paper. *J. Soil Mech. Found. Div. Jan. 1973. 1F, 6R. J. Geotech. Engng. Div. V100, N. GT8, 1974, 949–951. Int. J. Rock Mech. Min. Sci. Geomech. Abst.*, 11, 11, A230.
- Yousif, M.: 2019, Hydrogeological inferences from remote sensing data and geoinformatic applications to assess the ground water conditions: El-Kubanyia basin, Western Desert. *Egypt. J. African Earth Sci.*, 152, 197–214. DOI: 10.1016/j.jafrearsci.2019.02.003